Revolutionary Propulsion Concepts for Small Satellites

Steven R. Wassom, Ph.D., P.E.
Senior Mechanical Engineer
Space Dynamics Laboratory/Utah State University
1695 North Research Park Way
North Logan, Utah 84341-1947
Phone: 435-797-4600
E-mail: stevenw@mstar2.net

Abstract. This paper addresses the results of a trade study in which four novel propulsion approaches are applied to a 100-kg-class satellite designed for rendezvous, reconnaissance, and other on-orbit operations. The technologies, which are currently at a NASA technology readiness level of 4, are known as solar thermal propulsion, digital solid motor, water-based propulsion, and solid pulse motor. Sizing calculations are carried out using analytical and empirical parameters to determine the propellant and inert masses and volumes. The results are compared to an off-the-shelf hydrazine system using a trade matrix "scorecard." Other factors considered besides mass and volume include safety, storability, mission time, accuracy, and refueling. Most of the concepts scored higher than the hydrazine system and warrant further development. The digital solid motor had the highest score by a small margin.

Introduction

Aerospace America[1] recently provided some interesting data on the number of payloads proposed for launch in the next 10 years. In the year 2000 there was a 68% increase in the number of proposed payloads weighing less than 100 kg, a 67% increase in the number of proposed military payloads, and a 92% increase in the number of proposed reconnaissance/surveillance satellites. There are also several key government programs underway (TechSat21, XSS-10, XSS-11, ASTRO/Orbital Express) focused on developing enabling technologies for small satellite rendezvous, reconnaissance, on-orbit operations, and refueling. Collectively, this points to an important need to improve propulsion for small satellites in key areas, such as toxicity, safety, energy density, on-orbit storage, and ease of refueling, while maintaining performance and mission flexibility.

Current propulsion systems for attitude control, station-keeping, or orbit transfer typically involve propellants such as hydrazine (N_2H_4) that are toxic and/or have low energy density. Four new propulsion concepts are being developed that may offer significant advantages. The concepts are known as Solar Thermal Propulsion (STP), Water-Based Propulsion (WBP), the Digital Solid Motor (DSM), and the solid pulse motor.

Objective

The purpose of this effort was to compare the propulsion concepts to a state-of-the-art (SOTA) hydrazine system, as applied to a notional 100-kg satellite designed for rendezvous with other objects.

Basic Description of Concepts

Solar Thermal Propulsion (STP)

Solar Thermal Propulsion (STP) uses the sun's energy to heat a low molecular weight fuel such as hydrogen or ammonia. The thermal energy stored in the hot fuel is then converted to kinetic energy by expansion through a diverging nozzle. This results in a high efficiency (800 – 1,000 sec Isp) low thrust propulsion system. Spacecraft propelled using STP systems have been proposed for orbital transfer, interplanetary, and other missions. Much significant research for this approach has been previously performed and reported[2].

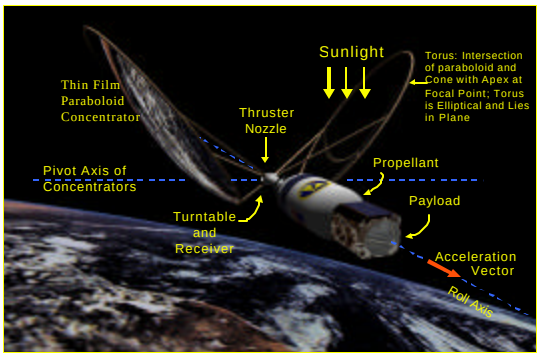

Figure 1. Artist's Concept of STP System

Copyright © 2001 by ATK Thiokol Propulsion Corp. Published by the American Institute of Aeronautics and Astronautics, Inc. with permission.
Approved for public release; distribution unlimited.

Figure 1 shows a conceptual view of a solar thermal rocket on orbit, featuring inflatable solar concentrators supported by inflated and rigidized struts. The concentrating mirrors are elliptical because geometrically they are actually opposing off-axis "slices" of a paraboloid whose axis points at the sun and whose focal point corresponds to the location of the engine.

Under Integrated High Payoff Rocket Propulsion Technology (IHPRPT) funding, The Air Force Research Lab (AFRL) at Edwards AFB has sponsored a key program over the last 4 years to demonstrate the technological readiness and performance of an inflatable solar thermal propulsion system. Progress thus far includes the following accomplishments:

- Component trade studies completed
- Rapid software prototyping and hardware-in-the-loop test system installed and verified
- Inflation control system designed, fabricated, and tested in both ambient and space environments
- Sun sensors for sun tracking system fabricated and tested
- Subscale integrated system fabricated and deployed in space environment
- Modal testing of subscale inflatable concentrator completed in ambient conditions
- Development, fabrication, and deployment testing of a full-scale concentrator
- Development and testing of the hexapod platform for focusing the concentrator
- Engine design and development
- Test stand design

Figure 2 shows the results of a deployment test using a 2-by-3-meter inflatable concentrator. The program will culminate in a full-up integrated proof-of-concept ground test later this year. This will demonstrate that the technology is ready for development of the flight hardware for the AFRL Solar Orbital Transfer Vehicle (SOTV) program.

The NASA Technology Readiness Level (TRL) for STP is estimated to be 4. NASA has used the TRL concept for many years to compare the maturities of technologies[3]. The component that is in the earliest stages of development is the optical system for sensing the focal spot and feeding the data to the hexapod focus control actuators.

Water-Based Propulsion (WBP)

WBP is described schematically by Figure 3[4]. Electrical power from the solar array is used to electrolyze water, converting it into hydrogen and oxygen propellant and electrochemically pumping it to a high storage pressure (2000 psi). This propellant can then be either ignited to produce thrust at ~400 sec Isp, or can be recombined in a fuel cell (2-5 times the energy density of the best batteries) to generate electrical power for the spacecraft bus. Cold gas from the pressurized tanks can also be used for attitude control thrusters. The electrolysis and fuel cell functions can be performed either by separate dedicated cell stacks, or can be combined in a new technology known as the Unitized Regenerative Fuel Cell (URFC). Since the pressurized gasses are produced on-orbit, WBP is totally inert and non-hazardous at launch. The bus structure could be hollow to serve as the gas storage repository. Mission and payload analyses have shown that WBP offers competitive propulsion performance to conventional state-of-the-art technologies, while its other attributes of non-toxicity, refuelability, and long-term high-energy storage make it superior for many applications. A working prototype has been built and tested. The TRL has been estimated to be 4[5].

Figure 2. Subscale STP Deployment Test

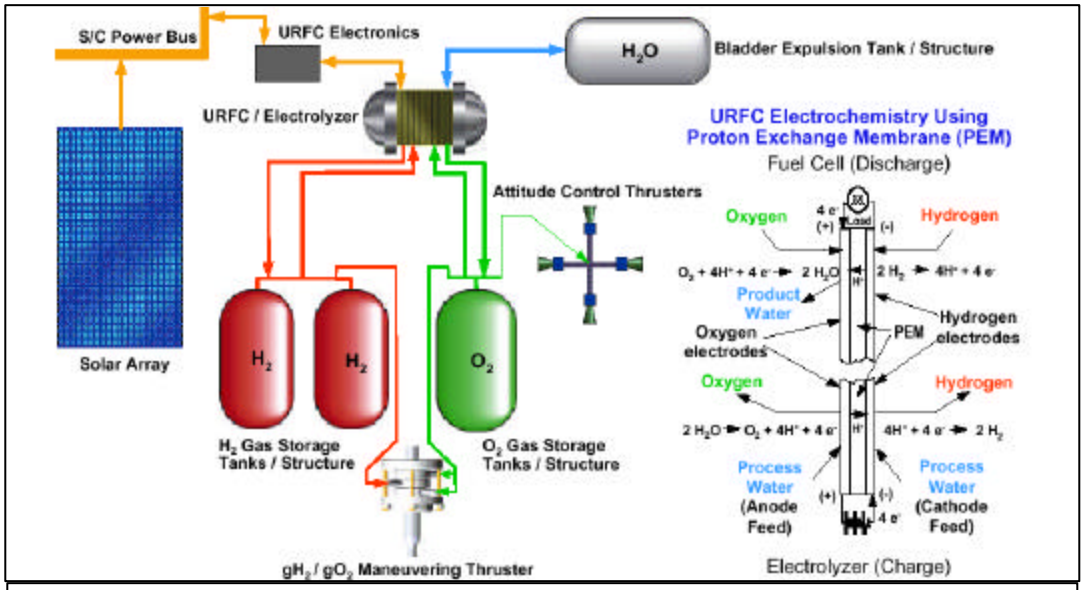

Figure 3. Water-Based Propulsion Schematic

Digital Solid Motor (DSM)

Solid propellant has significantly higher energy density than liquid propellant for chemical energy storage. The challenge lies in releasing the energy in throttleable, controllable amounts. In a concept first proposed by Robert H. Goddard over 85 years ago[6] (Fig. 4), small pellets of solid propellant are repeatedly loaded into a chamber and ignited, with the combustion products being expelled through a nozzle. This is very similar to an automatic gun, including the ease of reloading. By varying the duration of the bursts and the delay time between bursts, any level of control can be achieved down to a single impulse bit. Preliminary transient ballistic analyses show that thrust level and minimum impulse bit are competitive with liquid thrusters. Early system sizing studies indicate that the energy density can be better than liquid thrusters. These features combine with the low toxicity and ease of handling to result in a superior propulsion and power system. In 2000, a patent application was filed and a working prototype was successfully built and tested. Future efforts are being directed to a smaller, more compact, high-speed mechanism. The TRL of this concept is also 4.

Solid Pulse Motor

The pulse motor concept (Figure 5) is not new, having been developed extensively to the point of production, mainly for tactical missiles. Two or more discrete solid propellant grains are separated inside the motor case by a frangible barrier or bulkhead that can withstand the combustion pressure in one direction only. Thus, the aftmost pulse is ignited first, after which a coast period

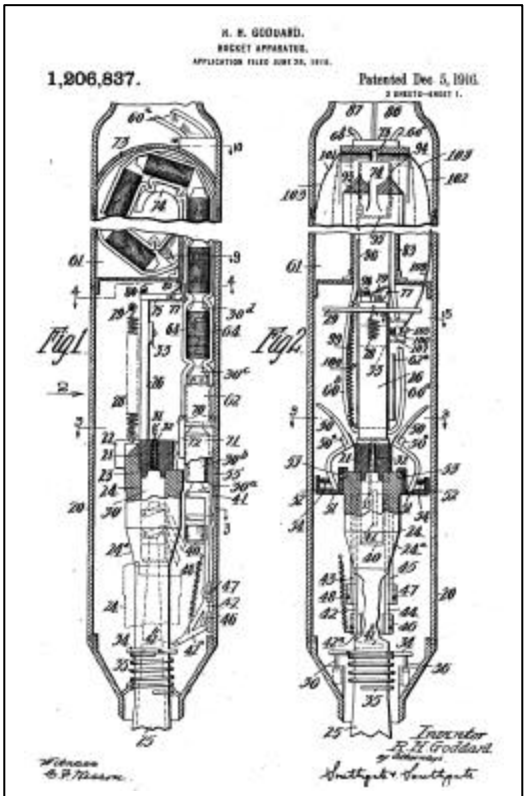

Figure 4. Goddard Concept for Digital Solid Motor

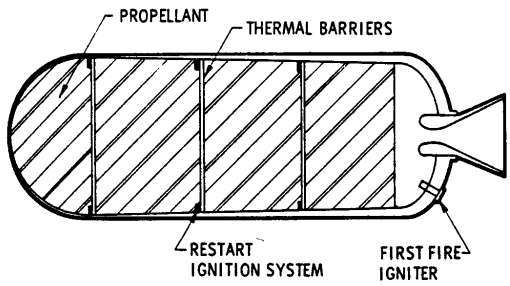

Figure 5. Pulse Motor Schematic

occurs, followed by the ignition of the forward pulse(s). In essence, this is the combination of a perigee and apogee kick motor in one package. The lack of ability to vary the delta-V of each pulse could be compensated by a guidance algorithm that makes use of the principle that any rendezvous trajectory can be chosen between two orbits, provided it has sufficient energy to intersect both. An implicit solution of Lambert's equations could be used to generate a look-up table that would match the delta-V's of the pulses to the correct transfer orbit. Essentially, any energy greater than that required for a Hohmann-type transfer would be wasted.

Two- and three-pulse motors are the most extensively developed. In fact, a two-pulse motor was recently used in a successful exo-atmospheric flight test[7]. Thus, its TRL would be 8. However, since the envisioned mission would involve 2 different orbit transfers, a minimum of 4 pulses would be required. The TRL of a single 4-pulse motor would be lower due to lack of development and demonstration. Another solution would be to have two 2-pulse motors packaged together, either side-by-side or in-line. However, the side-by-side arrangement would induce a large disturbing moment, unless a mechanism was used to translate each motor into position. The in-line arrangement would require the jettison of the aft motor and possibly the positioning of the new motor. A TRL of 4 is suggested for the pulse motor approach. Even though the motor itself is more mature than the other approaches, the positioning mechanism and guidance scheme would require some development.

Approach

The approach taken was to size each of the propulsion systems and perform a trade study by quantifying the following parameters for each system:

Payload Capability
Packaging Volume
Safety (Toxicity, Hazards)
Long-term Storability
Mission Time
Refueling Capability
Accuracy

The first step was to define the notional satellite and mission requirements. Several sources were consulted that seemed to represent the current high interest in small satellite on-orbit operations, such as rendezvous, reconnaissance, and refueling. A mission statement was formulated:

Mission Statement: Rendezvous with an existing space object, circumnavigate and image the object, and then repeat with a different object.

The mass of the satellite was chosen to be a maximum of 100 kg. The delta-V requirement was separated into a divert requirement of 600 m/sec and an attitude control system (ACS) requirement of 400 m/sec.

Although some of the propulsion concepts may also be applicable to ACS, the scope of this trade was restricted to divert propulsion. Thus, for ACS, an advanced pulsed-plasma-thruster approach was chosen similar to that currently being flown on the EO-1 spacecraft[8]. Assuming an Isp of 1000 sec and a propellant mass fraction of 0.4, the mass of the ACS system for a 100 kg spacecraft was calculated to be 10 kg, of which 4 kg is the propellant.

The weight breakdown for the spacecraft payload was as shown in Table 1.

Table 1. Microsat Payload Mass Summary (kg)

Sensors	20
Attitude Control System (ACS)	10
Structure & mechanisms	15
Power (PVA, batteries)	10
Attitude determination	3
Command & data handling	2
Communications	2
Margin	9.5
Total	71.5

The desired thrust level was initially chosen to be high at 445 N for several reasons. First, it provides a nearly ideal impulsive thrust for high efficiency with negligible gravity losses. Second, for the baseline system and most of the other systems, the sensitivity of the engine mass to thrust level is low (ranging from 0.004 kg/N to .006 kg/N), and thus the sensitivity of

total system mass to thrust level is even lower. One exception was the STP system with a high engine specific mass of 1 kg/N. As the study progressed, the importance of the thrust level and thrust-time profile was quantified and will be discussed later.

Each propulsion system was sized so that the payload fraction, propulsion component mass fractions, and packaging volume could be quantified. The sizing calculations were carried out in mass fractions so that they could be applied to any combination of payload and delta-V, not just the case mentioned above. Thus, the total mass of the vehicle could be determined by dividing the payload mass by the payload mass fraction, and then the propulsion component masses could be calculated by multiplying the total mass by the component mass fractions. Both analytical and empirical values were used, as explained in more detail in each section below.

Baseline Hydrazine System Sizing

The baseline hydrazine system was first sized. Crucial propellant and engine parameters were derived from published values for off-the-shelf (OTS) components:

Propellant Density $rho_p := 1000 \cdot \frac{kg}{m^3}$

Specific Impulse $I_{sp} := 235 \cdot sec$

Engine Specific Mass $m_e := 0.0044 \frac{kg}{N}$

The thrust-to-weight ratio was established to provide 445 N thrust for a 100-kg microsat:

$$TW := 0.45$$

The titanium tank fraction (inert mass/propellant mass) was caculated from a linear regression of OTS tanks versus typical delta-V capability:

$$m_t := -0.000017647 \frac{sec}{m} \cdot DV + 0.1706 \qquad m_t = 0.16$$

The calculations for payload fraction and propulsion mass fraction then proceeded as follows:

Final-to-Initial Mass Ratio $MR := e^{\frac{-DV}{g \cdot I_{sp}}}$

$$MR = 0.771$$

Propellant Mass Fraction $MF_p := 1 - MR$

$$MF_p = 0.229$$

Tank Mass Fraction $MF_t := m_t \cdot MF_p$

$$MF_t = 0.037$$

Engine Mass Fraction $MF_e := TW \cdot m_e \cdot g$

$$MF_e = 0.019$$

Propulsion System Mass Fraction

$$MF_{ps} := \frac{MF_p}{MF_p + MF_t + MF_e}$$

$$MF_{ps} = 0.803$$

Payload Fraction

$$MF_{pl} := 1 - MF_p - MF_t - MF_e$$

$$MF_{pl} = 0.715$$

Thus, for a SOTA 100-kg microsat using hydrazine propulsion, the payload is exactly as shown in Table I,

$$M_{pl} := 100 \cdot kg \cdot MF_{pl}$$

$$M_{pl} = 71.5 kg$$

and the propulsion system mass is 28.5 kg.

The volume of the propulsion system was taken to be primarily the tank volume, which is the largest component. The tank was assumed to have a gas-filled bladder to expel the propellant. Assuming an initial pressure of 400 psi and a final pressure of 100 psi, from the ideal gas law, the tank volume is related to the propellant volume by the relationship

$$V_t := \frac{100 \cdot kg \cdot MF_p}{rho_p} \cdot \left(\frac{400 \cdot psi}{400 \cdot psi - 100 \cdot psi} \right)$$

$$V_t = 0.031 m^3$$

Digital Solid Motor Sizing

Next, the DSM was sized. The DSM propellant and thruster parameters were estimated from recent ATK Thiokol Propulsion research and development efforts:

Propellant Density $rho_p := 1745 \cdot \frac{kg}{m^3}$

Specific Impulse $I_{sp} := 300 \cdot sec$

Engine Specific Mass $m_e := 0.005 \cdot \frac{kg}{N}$

The thrust-to-weight ratio was the same as for hydrazine:

$$TW := 0.45$$

The magazine fraction (inert mass/propellant mass) was estimated from a linear regression of delta-V capability, based on solid model designs and an OTS machine gun that uses caseless propellant cartridges:

$$m_m := -0.0000529 \frac{sec}{m} \cdot DV + 0.4618$$

$$m_m = 0.43$$

The calculation procedure was essentially the same as for hydrazine, but with the tank mass fraction being

replaced by the magazine mass fraction. The calculation results were:

Final-to-Initial Mass Ratio $MR = 0.816$

Propellant Mass Fraction $MF_p = 0.184$

Magazine Mass Fraction $MF_m = 0.079$

Engine Mass Fraction $MF_e = 0.022$

Propulsion System Mass Fraction $MF_{ps} = 0.645$

Payload Fraction $MF_{pl} = 0.714$

Thus, the total satellite mass was $M_{tot} = 100.1\,kg$

This is very close to the baseline hydrazine system. The low mass fraction of the DSM propulsion system at 0.645, compared to the hydrazine system at 0.8, is offset by the higher specific impulse.

The volume of the DSM propulsion system was taken to be primarily the propellant magazine volume. Assuming that the magazine material is similar to the density of the propellant, and that the propellant cartridges are of a rectangular shape like the machine gun to maximize the packing density, the volume was calculated as

$$V_t := \frac{M_{tot} \cdot (MF_p + MF_m)}{rho_p}$$

$$V_t = 0.015\,m^3$$

Solid Pulse Motor Sizing

The pulse motor parameters were estimated from extensive development and testing of similar solid propellant pulse motors:

Specific Impulse $I_{sp} := 285 \cdot sec$

Propellant Density $rho_p := 1820 \cdot \frac{kg}{m^3}$

The ratio of inert mass to propellant mass was estimated from a linear regression of delta-V capability, based on designs of production-status space motors:

$$m_i := -0.00005788 \frac{sec}{m} \cdot DV + .2847$$

$$m_i = 0.25$$

The calculations for payload fraction and propulsion mass fraction then proceeded similar to the hydrazine system, with the difference that there are no separate tank or engine components, and all inert components (nozzle, case, insulation) are lumped into the inert fraction. The results of the calculations were

Final-to-Initial Mass Ratio $MR = 0.807$

Propellant Mass Fraction $MF_p = 0.193$

Inert Mass Fraction $MF_i = 0.048$

Propulsion System Mass Fraction $MF_{ps} = 0.8$

Payload Fraction $MF_{pl} = 0.759$

Thus, the total satellite mass is $M_{tot} = 94.3\,kg$

This is better than the baseline hydrazine system. The high 0.8 mass fraction of the pulse motor is enhanced by the high specific impulse.

The volume of the pulse motor propulsion system was calculated using a volumetric efficiency of 0.7:

$$V_t := \frac{M_{tot} \cdot MF_p}{0.7 \cdot rho_p}$$

$$V_t = 0.014\,m^3$$

Solar Thermal Propulsion Sizing

Sizing the STP system was somewhat more involved because of the addition of the concentrating mirrors to the system, and the necessity of calculating the resulting concentrator mass fraction. The creation of the mirror geometry shown in Figs. 1 and 2 is clarified by a discussion of Figure 6. First, a parabola is defined with its axis pointing at the sun and the focus at the location of the engine. The parabola is then revolved about its axis, and the resulting solid paraboloid is cut on both sides by a plane defined by the angles shown. This creates 2 lenticulars that have elliptical shapes and cast circular shadows. The sun's rays are reflected by the lenticulars into the engine. It is evident from the diagram and equations that the amount of solar energy captured is determined by the focal length and the angles that define the cutting plane (note that θ is defined as a half-angle about the ray defined by ϕ). A larger value for ϕ results in a larger aperture, but then the exhaust from the engine may jeopardize the lenticulars. The angular values shown are typical of the state of the art and represent a good compromise. If the angles are held constant, then the aperture R and the solar power are proportional to the focal length f.

The STP system parameters were taken from the substantial work performed over the last several years under the aforementioned IHPRPT program. Two different propellants were examined; liquid hydrogen (LH2) and ammonia (NH3). First, the NH3 system will be sized:

$$I_{sp} := 400 \cdot sec$$

$$rho_p := 600 \cdot \frac{kg}{m^3}$$

$$MR := e^{\frac{-DV}{g \cdot I_{sp}}}$$

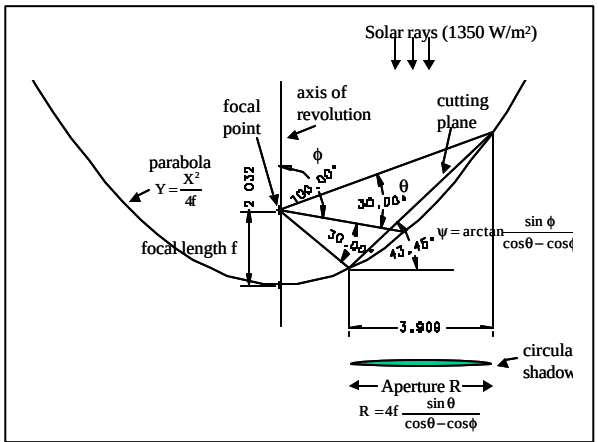

Figure 6. Solar Concentrator Geometry

$$MR = 0.858$$

The thermodynamic efficiencies of the concentrator and engine in converting the solar power into thrust are defined from the IHPRPT program to be

$$eta_c := 0.6$$

$$eta_e := 0.35$$

The specific mass of the concentrator is defined as the ratio of the mass of all of the components for 2 concentrators (lenticular, supporting torus, struts, focus control system, and inflation control system) to the amount of solar power reflected. The IHPRPT program studies have estimated this for a flightweight system to be

$$m_c := 0.00055 \frac{kg}{watt}$$

The thrust for an STP system is low to keep the size of the concentrator and heat-exchanger engine to a reasonable value. This can be seen by equating the power out of the nozzle (which is one-half the thrust times the specific impulse) to the solar power reduced by the engine and concentrator efficiencies, and then forming the ratio of the thrust to the solar power (i.e., N/watt):

$$T_s := \frac{eta_c \cdot eta_e}{0.5 \cdot g \cdot I_{sp}}$$

$$T_s = 1.07 \times 10^{-4} \frac{N}{watt}$$

Thus, a thrust of 448 N like the previous systems would require a very large solar input and concentrator aperture area:

$$W_{sun} := \frac{448 \cdot N}{T_s}$$

$$W_{sun} = 4.186 \times 10^6 W$$

Concentrator mass $M_c := W_{sun} \cdot m_c$

$$M_c = 2.302 \times 10^3 kg$$

The engine specific mass is also high because it uses heavy refractory metals to handle the extreme temperatures, and also incorporates a secondary concentrator to gather the stray energy and increase the efficiency:

$$m_e := 1 \cdot \frac{kg}{N}$$

So the thrust-to-weight ratio was set to try to achieve a 1-N thrust for a 100-kg microsat:

$$TW := 0.001$$

The concentrator mass fraction was formed by again comparing the power out of the nozzle to the solar power throughput, but using the concentrator specific mass and the thrust-to-weight ratio to form the ratio of concentrator mass to total spacecraft mass:

$$MF_c := \frac{0.5 \cdot g \cdot TW \cdot g \cdot I_{sp} \cdot m_c}{eta_c \cdot eta_e}$$

$$MF_c = 0.05$$

The tankage and propellant mass fractions for the NH3 and the LH2 cases were carried out differently because of the nature of the propellants. NH3 can be stored in a similar manner to hydrazine, in a pressurized tank with an expulsion bladder. LH2, on the other hand, must be stored in a cryogenic tank that maintains the liquid state using a complex thermal management system. Also, a significant amount of extra LH2 must be carried on board to make up for losses.

Thus, the NH3 tank fraction (inert mass/propellant mass) was calculated similar to the hydrazine system by taking the linear regression used for hydrazine and dividing it by 2 to reflect the assumed use of an advanced composite tank compared to titanium :

$$m_t := \frac{-0.000017647}{2} \cdot \frac{sec}{m} \cdot DV + \frac{0.1706}{2}$$

$$m_t = 0.08$$

The subsequent calculations were then like before, but with the addition of the concentrator mass fraction. The results were:

Propellant Mass Fraction $MF_p = 0.142$

Tank Mass Fraction $MF_t = 0.011$

Engine Mass Fraction $MF_e = 9.81 \times 10^{-3}$

Propulsion System Mass Fraction $MF_{ps} = 0.665$

Payload Fraction $MF_{pl} = 0.787$

Thus, the total satellite mass is $M_{tot} = 90.9 kg$

This is lighter than the baseline hydrazine system. The low mass fraction of the STP propulsion system, 0.665,

compared to the hydrazine system at 0.8 is offset by the higher specific impulse.

The volume of the NH3 STP propulsion system, as in the hydrazine case, was characterized by primarily the tank volume. (The inflatable solar concentrators typically take up much less volume than the tank when in their packaged and undeployed state.) Assuming the same pressure blowdown system as the hydrazine, the volume is

$$V_t = 0.029 m^3$$

It is also interesting to calculate the solar input power required and the resulting size of the deployed concentrators. This is done by dividing the power out of the nozzle by the concentrator and engine efficiencies:

$$W_{sun} := \frac{0.5 \cdot M_{tot} \cdot TW \cdot g \cdot I_{sp} \cdot g}{eta_e \cdot eta_c}$$

$$W_{sun} = 8.331 \times 10^3 W$$

Then the minor diameter of each elliptical mirror, which is also the aperture R shown in Fig. 6, is found by dividing the solar power by 2 (for each side), then dividing it by an insolation of 1350 W/m2 for LEO to get the area, then calculating the diameter:

$$R := \sqrt{\frac{W_{sun}}{2 \cdot 1350 \cdot \frac{watt}{m^2}} \cdot \frac{4}{\pi}}$$

$$R = 1.982 m$$

The major elliptical diameter is found by dividing the minor diameter by cosine of the angle shown in Fig. 6:

$$a := \frac{R}{\cos(43.45 \cdot deg)}$$

$$a = 2.73 m$$

This is very near the size of the concentrator shown in Fig. 2 that has been tested in ambient and vacuum environments.

Next, the STP system using LH2 propellant was sized using essentially the same procedure:

$$I_{sp} := 800 \cdot sec$$

$$rho_p := 64 \cdot \frac{kg}{m^3}$$

$$MR = 0.926$$

$$MF_c = 0.101$$

The LH2 tank fraction is based on an advanced graphite composite cryogenic tank with a metallic liner and a propellant management system that was recently successfully tested in a NASA vacuum chamber:

$$m_t := 0.25$$

The LH2 propellant mass fraction included 20% extra to make up for losses:

$$MF_p := 1.2 \cdot (1 - MR)$$

$$MF_p = 0.088$$

The calculations for payload fraction and propulsion mass fraction then proceeded as before:

Tank Mass Fraction $MF_t = 0.022$

Engine Mass Fraction $MF_e = 9.81 \times 10^{-3}$

Propulsion System Mass Fraction $MF_{ps} = 0.4$

Payload Fraction $MF_{pl} = 0.779$

Thus, the total satellite mass was $M_{tot} = 91.8 kg$

This is lighter than the baseline hydrazine system. The low mass fraction of the STP propulsion system, 0.4, compared to the hydrazine system at 0.8 is offset by the higher specific impulse.

The volume of the STP propulsion system using LH2 was taken to be primarily the propellant volume.

$$V_t := \frac{M_{tot} \cdot MF_p}{rho_p}$$

$$V_t = 0.127 m^3$$

This is very large because of the low density of LH2.

The solar input power is

$$W_{sun} = 1.683 \times 10^4 W$$

The aperture diameter (and ellipse minor diameter) is

$$R = 2.817 m$$

The major elliptical diameter is

$$a = 3.88 m$$

Water-Based Propulsion Sizing

The WBP system is the most challenging to size, since it has more components than the other systems. These include additional tankage (initially empty) for storing the generated H2 and O2 gasses, the stack of URFC cells, and extra photovoltaic array (PVA) capability for electrolyzing the water.

The WBP system parameters were taken from the substantial work performed over the last several years under studies carried out by Lawrence Livermore National Labs[9] (also see Refs. 3 and 4):

Specific Impulse $I_{sp} := 390 \cdot sec$

Density of Water Propellant $rho_p := 1000 \cdot \frac{kg}{m^3}$

The oxygen-to-fuel ratio of O2 to H2 in the thruster was chosen to be near-stoichiometric at 8:1. This then results in the mass of the total H2 that must be generated of

$$\frac{m_{H2}}{m_{H2O}} := \frac{1}{1+8}$$

One important parameter is the mission time, since the electrolysis process depends on the available input power from the PVA and the time. It must be kept in mind that this mission time is the time required to do the 2 orbit transfers. In actual practice, the 2 transfers would be split up by the time to circumnavigate and image the target. This study examined a range of mission times. As an example,

$$t_{miss} := 15 \cdot day$$

Then the required rate of generation of the H2, assuming that an average of 92% of each orbit is in the sun, is

$$mdot_{H2} := \frac{m_{H2}}{0.92 \cdot t_{miss}}$$

This gas generation rate, from Faraday's law of electrolysis, is also a function of the net current through the cell stack and the number of cells:

$$mdot_{H2} := n_{cell} \cdot i_{net} \cdot farad$$

where ncell is the number of cells and "farad" is Faraday's constant:

$$n_{cell} := 16$$

$$farad := 0.0008953 \frac{\frac{kg}{day}}{amp}$$

The net current is an empirical fraction of the total current, due to losses that are a function of the cell area, the current density, and the pressure to which the cells electrochemically pump the gas (2000 psi is the currently accepted achievable pressure):

$$i_{net} := 0.366 \frac{W_{in}}{V_{bus}}$$

where Win is the input PVA power and Vbus is the bus voltage:

$$V_{bus} := 28 \cdot V$$

Combining the above relationships results in the ratio of input power to propellant mass that must be electrolyzed:

$$W_p := \frac{V_{bus} \cdot \left(\frac{1}{1+8}\right)}{farad \cdot 0.92 \cdot t_{miss} \cdot n_{cell} \cdot 0.366}$$

$$W_p = 43 \frac{watt}{kg}$$

The ratio of URFC mass to propellant mass is also an empirical factor of the number of cells, the current density in the cell, and the input power:

$$m_{URFC} := 0.006 \frac{kg}{watt} \cdot W_p$$

$$m_{URFC} = 0.258$$

The tank fraction is composed of a system of tanks: a tank to store the unpressurized water, and tanks (initially empty) to separate and store the pressurized H2 and O2 resulting from electrolysis. The pressure tanks are sized based on the largest single delta-V burn required during the mission. For this study, it was assumed that the orbit transfers would be divided into equal sizes of burns; thus, the tanks are filled and emptied a predetermined number of "electrolyze-and-burn" (EB) cycles. Also, the volume of the O2 tankage is exactly half of the H2 tankage, since the O/F ratio is 8 and the ratio of the molecular weights is 16. Thus, it is assumed that there are 3 pressure tanks of equal volume: 2 for the H2 and 1 for the O2.

The mass of one tank is found using an empirical figure of merit known as "PV over W", which is the ratio of the tank pressure times the tank volume, divided by the tank weight. For a carbon fiber composite tank, this was assumed to be

$$PVW := 35560 \cdot m$$

This study examined the effect of varying the number of EB cycles; for example,

$$n_{eb} := 10$$

The ratio of the mass of a single tank to the mass of H2O propellant, assuming a 1.5 safety factor, is

$$\frac{m_{tank}}{m_{H2O}} := \frac{1.5 \cdot PV_{H2}}{2 \cdot n_{eb} \cdot g \cdot m_{H2O} \cdot PVW}$$

But from the ideal gas law (and including 10% margin in the tank),

$$PV_{H2} := 1.1 \cdot m_{H2} \cdot R \cdot T$$

Combining the above relations and assuming a temperature of 200 K gives the ratio of a single pressure tank mass to the propellant mass:

$$\frac{m_{tank}}{m_{H2O}} := \frac{0.215}{n_{eb}}$$

But this is just for one pressure tank; there are 3 tanks plus a water tank. Assuming that the water tankage fraction is 2% gives a total tankage fraction of

$$m_t := \frac{0.645}{n_{eb}} + 0.02$$

$$m_t = 0.085$$

The fractions for the URFC and tankage have now been determined; what remains is the extra PVA capability needed to generate the power for electrolysis.

Projections from government-funded programs in thin-film solar arrays give the anticipated power density of 150 watts/kg in a few years[10]. Thus, the ratio of extra PVA mass to propellant mass is

$$m_{PVA} := 0.0067 \cdot \frac{kg}{watt} \cdot W_p$$

$$m_{PVA} = 0.288$$

The thrust-to-weight ratio is the same as for hydrazine and DSM:

$$TW := 0.45$$

The engine fraction was taken from a demonstrated gas-gas thruster:

$$m_e := 0.00572 \cdot \frac{kg}{N}$$

The calculations for payload fraction and propulsion mass fraction then proceeded as before, but including the extra components:

Final-to-Initial Mass Ratio $MR = 0.855$

Propellant Mass Fraction $MF_p = 0.145$

Tank Mass Fraction $MF_t = 0.012$

Engine Mass Fraction $MF_e = 0.025$

URFC Mass Fraction $MF_{URFC} = 0.037$

PVA Mass Fraction $MF_{PVA} = 0.042$

Propulsion System Mass Fraction $MF_{ps} = 0.554$

Payload Fraction $MF_{pl} = 0.738$

Thus, the total satellite mass was $M_{tot} = 96.9\,kg$

This is lighter than the baseline hydrazine system. The low mass fraction, 0.55, compared to the hydrazine system at 0.8 is offset by the higher specific impulse.

The volume of the WBP system is a combination of the water tank, the URFC stack, and the pressurized gas tanks. From the ideal gas law, the O/F ratio, and the number of EB cycles, the volume of the pressurized tanks is

$$V_{ptanks} := \frac{0.01086 \frac{m^3}{kg} \cdot MF_p \cdot M_{tot}}{n_{eb}}$$

$$V_{ptanks} = 0.015\,m^3$$

The volume of the water tank is simply taken as the water volume itself. The volume of the URFC stack is the mass of the stack divided by an empirical stack density:

$$V_{stack} := \frac{MF_{URFC} \cdot M_{tot}}{1248 \cdot \frac{kg}{m^3}}$$

Thus, the total volume is

$$V_{tot} := V_{ptanks} + V_{stack} + \frac{MF_p \cdot M_{tot}}{rho_p}$$

$$V_{tot} = 0.03224\,m^3$$

The size of the system is influenced both by the number of EB cycles and the mission time. Figures 7 and 8 show plots of payload fraction and volume versus mission time for different EB cycles. The mission time has the greatest effect due to the large increase in size in the URFC stack and the extra PVA power required. The number of EB cycles has little effect on payload fraction, but does influence the volume. The combination of 30 EB cycles and 11 days was selected, since it results in a total spacecraft mass of 100 kg.

Effects of Thrust Profile on Mission Time, Rendezvous Accuracy, and Propellant

The low thrust level of the STP concept raised the issue of the effect of thrust level on the system sizing and performance. More specifically, it was important to determine the effect of thrust on mission time, rendezvous accuracy, and propellant requirement.

A simple study was performed in which the orbital equations of motion in a plane were integrated with different thrust levels, impulse bits, and burn times. It was assumed that the spacecraft is a point mass under the influence of gravity (inverse square law) and thrust, which is always aligned with the velocity vector (see Figure 9).

The equations of motion were derived to be

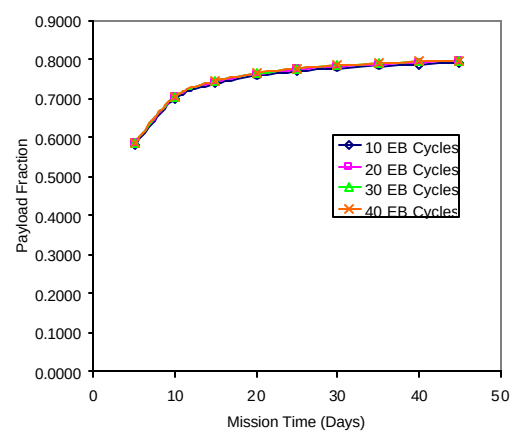

Figure 7. WBP Payload Fraction

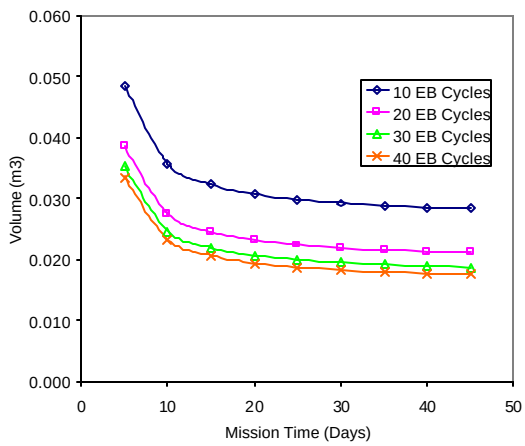

Figure 8. WBP Volume

$$\frac{du}{dt} := \frac{T \cdot \sin\phi}{m} - \frac{\mu}{r^2} + \frac{v^2}{r}$$

$$\frac{dv}{dt} := \frac{T \cdot \cos\phi}{m} - \frac{u \cdot v}{r}$$

$$\frac{dr}{dt} := u$$

$$\frac{d\theta}{dt} := \frac{v}{r}$$

$$\frac{dm}{dt} := \frac{-T}{g \cdot I_{sp}}$$

The goal was an elliptical transfer from a circular orbit of 390 km to an elliptical orbit with an apogee of 1270 km. The effects of different thrust profiles were compared to an ideal impulsive thrust. The initial conditions on the state variables were

r	6768 km
mass	100 kg
u	0 m/sec
v	7674.3 m/sec

Finite burns were centered at the perigee point, meaning that the initial condition on the true anomaly θ varied depending on the burn time and length of the burn arc. It was calculated as ½ of the initial angular velocity (v/r) times the burn time. Various thrust levels and burn times were used. For the very low thrust levels, multiple orbits were required, and so different burn arc lengths were tried.

An Isp of 300 sec was assumed. The well-known equation[11] for the first burn of a Hohmann transfer was used to calculate the delta-V for an ideal impulse:

$$\Delta V := \sqrt{\frac{\mu}{r_0}} \cdot \left(\sqrt{\frac{2 \cdot \frac{r_a}{r_0}}{1 + \frac{r_a}{r_0}}} - 1 \right)$$

The resulting delta-V was 231.3 m/sec, the propellant mass was 7.56 kg, and the transfer time was 0.85 hour (1/2 of one orbit).

In the case of the digital solid motor, the effect of minimum impulse bit was also included. Fig. 10 shows the accuracy of the apogee rendezvous as a function of propellant usage for an ideal impulsive thrust, and for square and sawtooth pulses for the DSM. The minimum impulse bit of the DSM was 3 g of propellant, which equated to 2 lbf-sec (8.9 N-sec). This made a difference of 390 m in the apogee.

This then posed the question: how much propellant would be then needed at apogee to complete the rendezvous? The force-free solution to Hill's equations for relative motion[12] were used to calculate the propellant mass required to make up the error. The results in Fig. 11 show that a relatively small mass is required. The results are sensitive to time, with 0.5 hour being nearly optimum.

Other thrust levels were used, ranging from to the 1-N thrust level of the STP concept up to 445 N. The results are shown in Fig. 12. It appears that the thrust can be reduced all the way down to 22-44 N before it starts to have a significant effect on propellant required or mission time. The biggest effect on mission time comes when multiple orbits are needed, which occurs at the very low thrust levels.

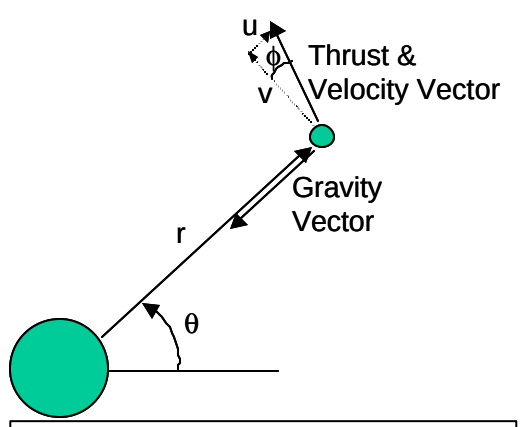

Figure 9. Model for Planar Trajectory Study

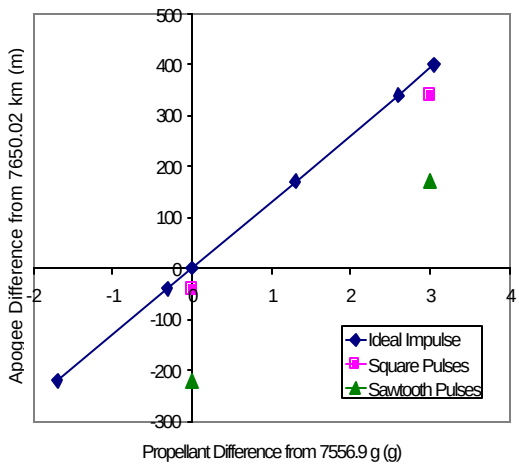

Figure 10. Effect of Impulse Bit on Apogee Accuracy

With these results, the mission time could then be quantified for the different concepts and included in the trade matrix. The total mission time was based on the usage of the entire delta-V budget of 600 m/sec. Since the trajectory study was for a single impulse at perigee, and the desired mission was for 2 rendezvous with different objects, the total mission would require at least 2 orbits (about 3.5 hours) for the high-thrust concepts. For the low-thrust STP concept, the 30-deg burn arc was chosen because of the small impact on extra propellant needed (about 5% or less). The trajectory was re-run for a delta-V of 150 m/sec, which is ¼ of the total delta-V, with the reasoning that the total mission is made up of 4 burn segments to rendezvous with the 2 different objects. The resulting time was about 26 hours, so the total mission would be about 104 hours.

It should be remembered and noted that the mission time for the WBP system is driven not by the thrust level, but rather by the time required for electrolysis.

Results

Table 2 shows the comparison of all of the systems for the payload mass of 71.5 kg and the divert delta-V

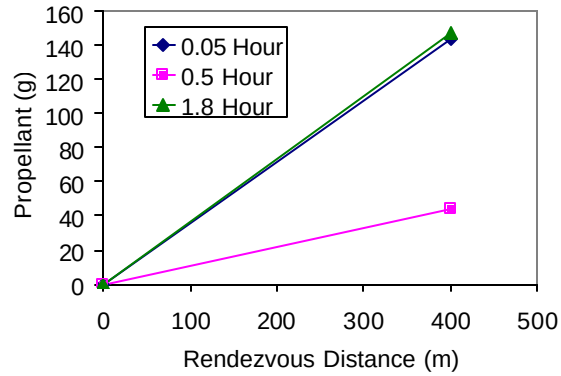

Figure 11. Rendezvous Propellant Requirement

requirement of 600 m/sec. The total system mass is not a tremendous discriminator, although the STP approach had the best payload fraction. The packaging volume, as determined by the volume of the largest component in the system, is more of a differentiator. Here the solid propulsion approaches (DSM and pulse) were the best due to their high propellant density.

These results raised the question of what the trade would look like for a wide range of delta-V's. Accordingly, the sizing calculations were repeated in spreadsheet form for delta-V ranging from 200 m/sec to 4000 m/sec.

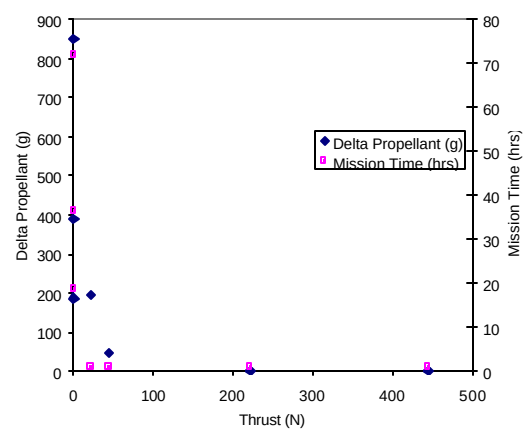

Figure 12. Effect of Thrust Level

Figure 13 shows the comparison of payload capability. At low delta-V's, the difference is small, but becomes much more pronounced at high delta-V's. The STP approach with liquid hydrogen provides the most capability. The propulsion mass fraction is compared in Fig. 14. Naturally, those concepts with the least amount of inerts generally provide the best mass fraction. The packaging volume comparison is shown in Fig. 15. The solid propellant concepts, the DSM and pulse motor, provide the best packaging volume. The STP with LH2 concept was omitted because the volume grows so rapidly with an increase in delta-V.

Table 2. Comparison of Sizing Results

	Baseline N2H4	STP w/NH3	STP w/LH2	DSM	WBP	Solid Pulse
Engine Mass (kg)	1.94	0.89	0.90	2.21	2.52	0.00
Propellant Mass (kg)	22.9	12.9	8.1	18.5	14.5	18.2
Tank or Magazine Mass (kg)	3.67	1.03	2.03	7.94	0.60	4.55
Concentrator Mass (kg)	N/A	4.6	9.3	N/A	N/A	N/A
URFC Mass (kg)	N/A	N/A	N/A	N/A	5.10	N/A
Extra PVA Mass (kg)	N/A	N/A	N/A	N/A	5.70	N/A
Payload Mass (kg)	71.5	71.5	71.5	71.5	71.5	71.5
Total Mass (kg)	100.0	90.9	91.8	100.1	99.9	94.3
Thrust (N)	442	0.9	0.9	442	441	416
Extra PVA Power (watts)	N/A	N/A	N/A	N/A	851	N/A
Volume (m3)	0.031	0.029	0.127	0.015	0.024	0.014
Propulsion Mass Fraction	0.80	0.66	0.40	0.65	0.51	0.80
Payload Mass Fraction	0.71	0.79	0.78	0.71	0.72	0.76
Approx. Mission Time (hrs.)	4	104	104	4	264	4

Trade Matrix

The trade matrix was formulated and scored as shown in Table 3. Originally, the technical risk of successful development was included in the trade matrix. However, a few reasons arose to justify eliminating it. First, each of the new concepts was assessed with the same TRL of 4. Second, there seem to be no insurmountable technical challenges to reaching flight-qualified systems, given time and budget.

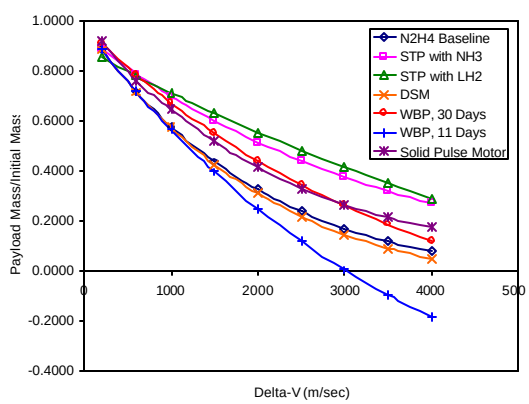

Figure 13. Payload Comparison

An effort was made to quantify each of the parameters for each of the concepts to enable scoring. Some of the parameters were directly quantifiable from the sizing and performance calculations. Others were much more subjective.

The best concept in each category was given a value of 10, and the others were scaled accordingly. Each of the categories was equally weighted for this example. Actual mission or program requirements would probably result in different weighting factors.

Payload and volume were taken directly from the results in Table 2, giving the best concept a score of 10 and scaling the others accordingly. Mission time score was calculated by scaling the mission times from Table 3 on a basis of 1 day or less. Safety was scored by consulting the hazards expert at ATK Thiokol Propulsion, who considered each propellant on the basis of toxicity, flammability, and reactivity. The rest of the categories were more subjective in nature. Ease of refueling was compared to the well-demonstrated liquid refueling of aircraft in flight or reloading a machine gun. Accuracy was based on the ability to throttle to a small impulse bit.

In general, the liquid systems tended to have higher scores in refueling because of the similarity to aircraft refueling, with the exception of cryogenic liquid

Table 3. Trade Matrix Scoring

	Baseline N2H4	STP w/NH3	STP w/LH2	DSM	WBP	Solid Pulse
Payload	9.1	10.0	9.9	9.1	9.1	9.6
Packaging Volume	4.7	5.0	1.1	9.4	6.0	10.0
Safety (Toxicity, Hazards)	2	5	6	5	10	6
Long-term Storability	10	10	2	10	10	10
Mission Time	10	2.3	2.3	10	0.9	10
Ease of Refueling	6	8	4	8	10	5
Accuracy (minimum bit)	9	10	10	8	9	7
Total	50.8	50.3	35.3	59.5	55.0	57.6

hydrogen. Also note that the DSM is given a high score in refueling because of the similarity to reloading a gun magazine. The liquid systems also had higher scores in accuracy because of the small impulse bit capability. However, they suffer from packaging volume due to the low propellant density.

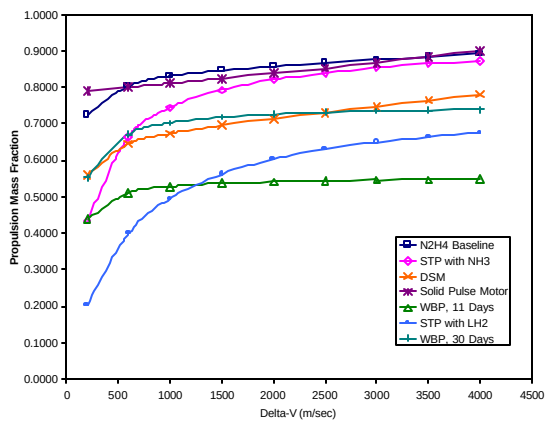

Figure 14. Propulsion Mass Fraction Comparison

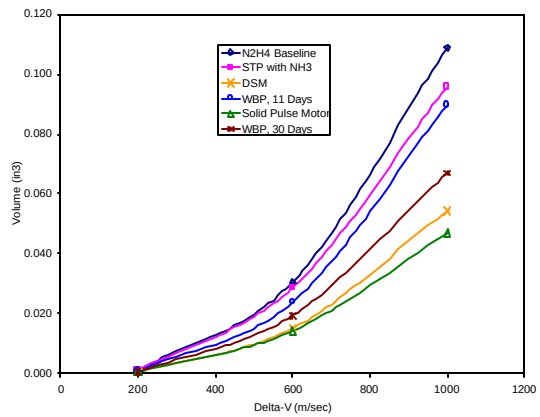

Figure 15. Volume Comparison

The baseline hydrazine system scores high in payload, mission time, and storability, but suffers from low scores in safety and packaging volume. The STP systems had the best accuracy because of the low thrust levels. However, the long mission times due to the low thrust may be undesirable. The DSM had the highest score overall. The WBP scored the highest in safety and storability, but is hampered by long mission times. The pulse motor had the best score in packaging, with the main area of concern being the refueling, which would probably consist of replacing the entire rocket motor. Accuracy is a concern because the guidance scheme using large predefined impulse bits is theoretically possible but yet to be demonstrated.

The STP system with liquid hydrogen did well in the payload and accuracy categories, but suffered from low scores in the other categories. It was the only concept deemed unacceptable for storability, and also had the lowest score in packaging volume because of the low propellant density. However, from Fig. 12 it is evident that STP with LH2 can provide a significant increase in payload at high delta-V's, assuming that the packaging volume is available and storability is not an issue.

Conclusions

An approach to sizing and comparing new propulsion systems for application to small satellites has been demonstrated. Assuming equal weighting for the trade matrix categories, the new concepts of STP with ammonia propellant, DSM, WBP, and solid pulse motor show advantages over hydrazine propulsion and warrant further development. The STP concept using liquid hydrogen should probably be eliminated from further consideration for small satellites with low delta-V requirements.

Acknowledgments

This study was funded under internal research and development by ATK Thiokol Propulsion. The work was performed and documented while the author was employed there in the Systems Engineering organization. He gratefully acknowledges the support and confidence of his former management and co-workers in this effort.

References

1. "Space Mission Model: 2001-2010," Aerospace America, June 2001.
2. Lester, D. M., S. R. Wassom, J. C. Pearson, and M. R. Holmes, "Solar Thermal Propulsion IHPRPT Demonstration *Program*," AIAA-2000-5109, AIAA Space 2000 Conference and Expo, Long Beach, CA, 19-21 Sep 2000.
3. Mankins, John C., "Technology Readiness Levels: A White Paper," NASA Office of Space Access and Technology, 6 April 1995, also available at http://www.hq.nasa.gov/office/codeq/trl/
4. Mitlitsky, Fred et.al., "Water Rocket—Electrolysis Propulsion and Fuel Cell Power," AIAA-99-4609, AIAA Space Technology Conference, Albuquerque, NM, 28-30 Sep. 1999.
5. Mitlitsky, Fred et.al., "Integrated Modular Propulsion and Regenerative Electro-energy Storage System (IMPRESS) for Small Satellites," AIAA/USU Conference on Small Satellites, Logan, UT, 19 Sep. 1996.
6. Goddard, R. H., Patents 1,103,503; 1,191,299; 1,194,496; 1,206,837.
7. http://www.atk.com/releases2/2001-06-21-TSRM.htm#TopOfPage
8. http://spacescience.nasa.gov/osstech/sec22.htm
9. Mitlitsky, Fred et.al., "Applications of Water Refuelable Spacecraft: A Study Performed for DARPA/TTO," Agreement #99-G527, 5 Jan. 2000.
10. Stollard, M., "Satellite Technology and Conceptual Design," presented 10 Feb. 1999 at the TechSat21 Kickoff Meeting; also available at leanair4.mit.edu/docushare/dscgi/ds.py/GetRepr/File-36/html
11. Kaplan, Marshall H., *Modern Spacecraft Dynamics and Control*, p. 83, Equation (3.18)
12. Kaplan, Marshall H., *Modern Spacecraft Dynamics and Control*, p. 114, Equations (3.54), (3.55)